International Journal of Mass Spectrometry and Ion Processes, 58 (1984) 1–14
Elsevier Science Publishers B.V., Amsterdam – Printed in The Netherlands

54

A THRESHOLD PHOTOELECTRON–PHOTOION COINCIDENCE SPECTROMETRIC STUDY OF DIMETHYL ETHER (CH_3OCH_3) *

JAMES J. BUTLER **

Department of Chemistry, The University of North Carolina at Chapel Hill, Chapel Hill, NC 27514 (U.S.A.)

DAVID M.P. HOLLAND ***

Institute of Physical Science and Technology, University of Maryland, College Park, MD 20742 (U.S.A.)

ALBERT C. PARR

Radiation Physics Division, National Bureau of Standards, Washington, DC 20234 (U.S.A.)

ROGER STOCKBAUER

Surface Science Division, National Bureau of Standards, Washington, DC 20234 (U.S.A.)

(First received 13 July 1983; in final form 5 September 1983)

ABSTRACT

The technique of threshold photoelectron–photoion coincidence spectroscopy has been used to study the dissociation of state-selected dimethyl ether (CH_3OCH_3) cations. The crossover region (10.5–11.5 eV) of the breakdown curve for the lowest energy dissociation ($CH_3OCH_3^+ \rightarrow CH_3OCH_2^+ + H$) has been recorded for the first time using threshold photoelectron–photoion coincidence with variable ion residence time. No shift in the crossover point is detected for a change in residence time of 0.66–5.57 μs, indicating that the H loss dissociation is a fast ($k \geq 10^7$ s^{-1}) process. A calculated fit to the 5.57 μs data produces a threshold of 11.115 ± 0.010 eV at a temperature of 0 K. Information on higher energy fragmentations is obtained from the breakdown curve. The shape of the m/z 29 ion curve indicates that m/z 29 ions are being formed by at least two processes. At low energy, HCO^+ is the product of a secondary dissociation from the unstable H_3CO^+ (m/z 31) fragment ion. This dissociation is joined at higher energies by the secondary reaction of the H_2COH^+ (m/z 31) and $CH_3OCH_2^+$ (m/z 45) fragments to the HCO^+ ion.

---

* Dedicated to the memory of H.M. Rosenstock.

** Intergovernmental Personnel Act Appointee at the National Bureau of Standards, 1982–1983.

*** Present address: Science Research Council, Daresbury Laboratory, Daresbury, Warrington WA4 4AD, Gt. Britain.

0168-1176/84/$03.00

INTRODUCTION

The ionization and dissociation energetics of dimethyl ether (CH_3OCH_3) have been intensively studied over the last 26 years using spectroscopic [1], electron impact [2–10], and photoionization techniques [11–23]. The conclusions of these studies have greatly increased our understanding of the fragmentation of the dimethyl ether cation. However, several aspects of its gas phase ion chemistry remain either unanswered or unconfirmed. Clearly, the most controversial aspect of the dimethyl ether story has concerned the appearance energy (AE) and structure of the m/z 31 fragment ion. The appearance energy of this ion from dimethyl ether has been measured in several independent electron impact experiments [3–10]. The AE in these experiments has consistently fallen within the 11.0–12.5 eV energy range. In a photoionization experiment by Botter et al. [23], however, the AE for m/z 31 was measured at 13.35 eV. This large discrepancy was explained at the time as being due to the population by electron impact of a low energy optically forbidden ionic state of dimethyl ether which dissociates to m/z 31. Efforts to identify the structure of the m/z 31 ion have produced three isomers. The methoxide structure, H_3CO^+, was assumed to be the correct structure in early studies [4,7]. In later experiments [8,24–26], the protonated formaldehyde, H_2COH^+, and an H_2–HCO^+ complex structure were proposed as being correct. A collisional activation study by Dill et al. [24] has provided evidence that the ion has the protonated formaldehyde structure.

Recently, Bouma et al. [25] have performed ab initio molecular orbital calculations in an effort to elucidate the structure of the H_2COH^+ ion at threshold. They reported that the m/z 31 ion is formed with the H_2COH^+ structure following an isomerization of dimethyl ether$^+$ to the $CH_3OHCH_2^+$ structure. The $CH_3OHCH_2^+$ ion has been experimentally determined to be 42 kJ mol^{-1} more stable than $CH_3OCH_3^+$ [27].

In this study, we have examined the ionization and dissociation of state-selected dimethyl ether cations using the experimental technique of threshold photoelectron–photoion coincidence with variable ion residence time. We report here for the first time the complete breakdown curve from 10.5 to 18 eV and the threshold photoelectron spectrum from 9.5 to 19.5 eV. The results of our experiments examined in relation to those of previous studies enable us to determine the origins and onsets of the fragment ions.

EXPERIMENTAL

The threshold photoelectron spectrum and breakdown curve for dimethyl ether were obtained using the threshold photoelectron–photoion coincidence

spectrometer described previously [28–30]. Figure 1 shows schematically the spectrometer with its data acquisition electronics and data processing system. In the coincidence experiment, vacuum ultraviolet light produced by either a hydrogen many-line or helium Hopfield continuum light source is dispersed by a 1-m Seya–Namioka monochromator. The monochromatic light is used to photoionize a low pressure of gaseous sample in the source region of the spectrometer. Photoelectrons are accelerated by a weak (0.8 V cm^{-1}) electrostatic field toward the electron analyzer–detector system. The electron energy analyzer comprises an electron drift tube acting as a steradiancy analyzer followed by a 127° electrostatic sector analyzer. Voltages on this analyzer system are chosen so as to allow the passage principally of electrons formed with essentially zero kinetic energy. The form of the electron energy analyzer sampling function was determined during the course of the dimethyl ether experiments to be identical to that previously determined in ref. 28. The width of the function is 26 meV fwhm. The electron signal provides the start signal to the time digitizer and the trigger signal to the high voltage pulser. The output of the high voltage pulser is used to eject ions from the source region. Upon application of the pulse, ions are accelerated through the source, pass through a drift region, and are detected by the ion multiplier. Detection of the ion provides the stop signal to the time digitizer. The difference in time between start and stop signal is the ion time of flight and is a function of the mass and charge of the ion.

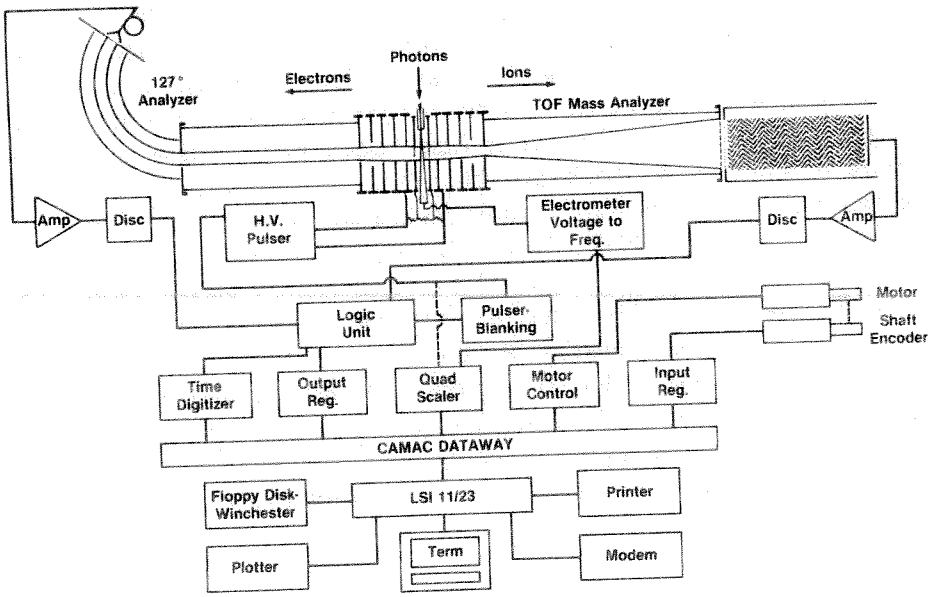

Fig. 1. Schematic of the coincidence spectrometer, electronics and data processing system.

For a study of kinetic shift effects, the time of application of the ejection pulse can be delayed by first passing the trigger to the high voltage pulser through a gate and delay unit (not shown in Fig. 1). In this manner, delays of the ion ejection pulse on the order of microseconds are realized and the time available for ionic fragmentation or isomerization in the source is increased.

In the photoelectron experiment, threshold electrons are counted in addition to the photons. The connection represented by the dotted line in Fig. 1 enables the electrons to be counted in this experiment.

The spectrometer is controlled in the coincidence and photoelectron experiments by an LSI 11/23 computer* with CAMAC instrumentation. A more detailed account of the automation of the spectrometer will be published in the near future.

The high resolution mass spectrometric studies were performed at NBS on a Varian-MAT 731 mass spectrometer operated at a resolution of 5000.

RESULTS

Threshold photoelectron spectrum

The threshold photoelectron spectrum of dimethyl ether is shown in Fig. 2(a). The adiabatic ionization potential is 10.025 ± 0.025 eV as interpreted from the maximum of the first band in the spectrum. This value is in agreement with several previously reported ionization potentials for dimethyl ether obtained by photoelectron [11,12,15,16,18,19,22], spectroscopic [1], and photoionization methods [23]. The first band of the photoelectron spectrum has been assigned as originating from the ionization of one of the non-bonding oxygen electrons [31]. The next four bands with vertical ionization potentials of 11.91, 13.43, 14.20 and 16.0 eV have also been assigned [31]. These bands are evident in the threshold photoelectron spectrum of Fig. 2(a).

A comparison of the HeI [31] and threshold photoelectron spectra of dimethyl ether between the energies of 10.5 and 11.5 eV clearly shows that the Franck–Condon gap between the first two bands in the threshold spectrum is not as deep as that in the HeI spectrum. This significant threshold electron signal is due to autoionization leading to the production of zero or near zero energy electrons. This autoionization process allows us to measure coincident ion signals in energy regions where the cross-section for direct photoionization as indicated by the HeI photoelectron spectrum is negligible.

---

* Certain commercial products are identified in this paper. This does not constitute an endorsement by the National Bureau of Standards.

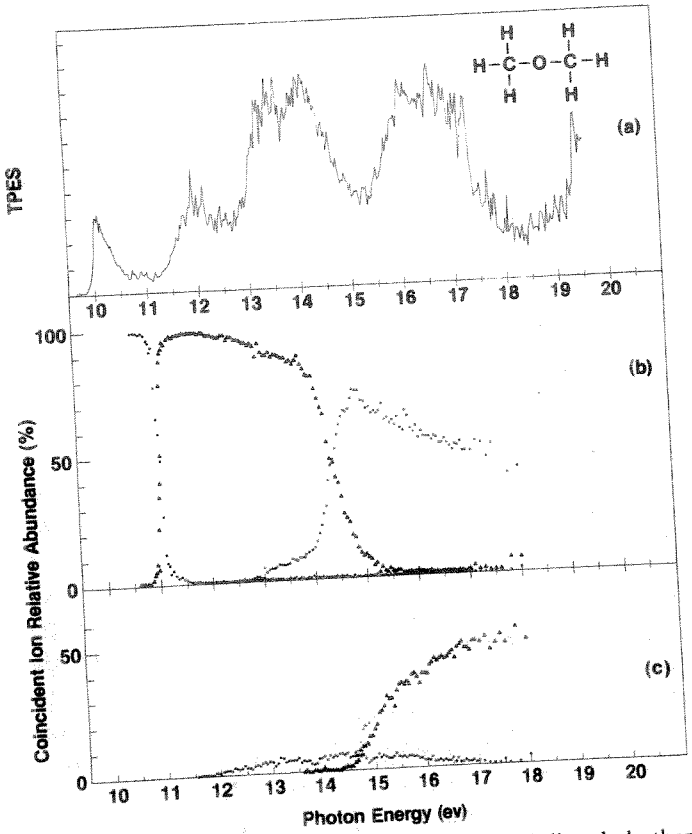

Fig. 2. (a) Threshold photoelectron spectrum of dimethyl ether. (b) Breakdown curves of ●, parent$^+$ ($CH_3OCH_3^+$); ▲, m/z 45 ($CH_3OCH_2^+$); and ○, m/z 29 (HCO^+). (c) Breakdown curves of ●, m/z 31 (H_2COH^+) and ▲, m/z 15 (CH_3^+).

Breakdown curve

The complete breakdown curve for dimethyl ether from 10.5 to 18 eV is shown in Fig. 2(b) and (c). The first ion to be formed in the ionic dissociation of dimethyl ether is the m/z 45 ion. In Fig. 2b, the rise of the m/z 45 curve corresponds to the fall of the parent m/z 46 curve, with the two curves crossing at an energy of approximately 11.0 eV. Interestingly, the energy region of the m/z 45 onset corresponds to that of the Franck–Condon gap in the threshold photoelectron spectrum of Fig. 2(a). The m/z 45 ion, therefore, is formed in this energy region by the dissociation of highly vibrationally excited dimethyl ether parent ions produced by autoionization. The second fragment ion from dimethyl ether is the m/z 31 ion whose curve is shown in Fig. 2(c). An AE(298) $\leq 11.85 \pm 0.10$ eV can be measured from

this curve. This AE and all AEs obtained from the ion curves of Fig. 2(b) and (c) are reported as upper limits due to the possible presence of kinetic shifts in the dissociations. In the energy region in which the m/z 31 ion curve rises, the m/z 45 curve decreases slightly but never crosses the m/z 31 curve. This indicates that, in this energy region, the m/z 31 ion is formed by a process competitive with that of the m/z 45 fragment ion. The third ion to be identified from the dimethyl ether breakdown curve is m/z 29 in Fig. 2(b). An AE(298) $\leq 12.85 \pm 0.10$ eV is measured from this curve. At 14.0 ± 0.1 and 14.9 ± 0.1 eV, the m/z 29 curve exhibits abrupt changes in slope which divide the curve into three sections: 12.85–14.0, 14.0–14.9 and 14.9–18 eV. The initial rise of the m/z 29 curve in Fig. 2(b) from 12.85 to 14.0 eV causes neither the m/z 45 or the m/z 31 ion curves to decrease to the extent of crossing the m/z 29 curve. This portion of the m/z 29 curve appears to be the result of a primary dissociation from m/z 46. Between 14.0 and 14.9 eV, the m/z 29 ion signal increases, the m/z 45 ion signal decreases, and the two ion curves exhibit a clear crossover point. This is evidence that, in this energy region, the m/z 29 ion is being produced in a secondary dissociation from the m/z 45 fragment. The slow decrease of the m/z 29 curve at photon energies higher than 14.9 eV corresponds to the increase in the m/z 15 ion curve of Fig. 2(c). From the m/z 15 curve, an AE(298) $\leq 14.4 \pm 0.1$ eV can be measured. The behavior of the m/z 29 and m/z 15 ion curves and the crossing of the rising m/z 15 curve by the falling m/z 45 curve indicates that m/z 15 is formed in a secondary dissociation from m/z 45 and is in competition with the m/z 29 dissociation.

Time-dependent breakdown curves of m / z 46 and m / z 45

The time dependence of the H-loss fragmentation channel was studied by recording the crossover region of the parent and m/z 45 breakdown curve at two different ion residence times. These results are presented in Fig. 3 for times of 0.66 and 5.57 μs. A comparison of the crossover points for the two residence times indicates that there is no shift in energy within the experimental limits of the crossover point. This means that the H-loss fragmentation occurs with a rate greater than or equal to 1×10^7 s^{-1} at its onset.

It has previously been shown [29,32] that, for fast dissociations in which there is no shift of the crossover point with time, the form of the parent and fragment breakdown curve should be describable by the convolution of a step function with an appropriate apparatus function and the rotational and vibrational thermal energy distributions. The results of these convolutions are shown in Fig. 3 as solid lines through the points of the 5.57 μs data. The apparatus function was given by the measured threshold photoelectron spectrum of Kr at the $^2P_{1/2}$ limit. The vibrational thermal distribution was

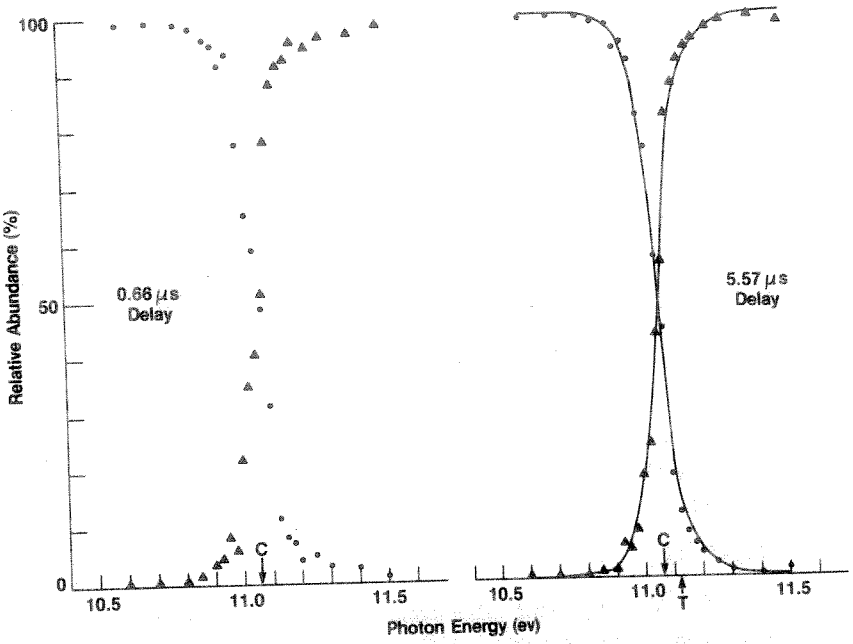

Fig. 3. Breakdown curve for the dissociation $CH_3OCH_3^+$ (●) → $CH_3OCH_2^+$ (▲)+H at 0.66 and 5.57 μs ion source residence times. The arrows labeled C and T indicate the photon energy at crossover (50% fragmentation) and the energy of the 0 K threshold, respectively.

calculated using the vibrational frequencies of dimethyl ether reported by Shimanouchi [33]. The rotational energy distribution was assumed to be that of a three-dimensional rotor. The superb fit of the calculated curve yields a 0 K fragmentation threshold of 11.115 ± 0.010 eV. The error in this measurement is a reflection of the small scatter in the data of the breakdown curve. This 0 K fragmentation threshold is in excellent agreement with a 0 K threshold of 11.12 ± 0.02 eV deduced by Botter et al. [23] in a study of the temperature dependence of the m/e 45 onset.

DISCUSSION

In this section, qualitative and quantitative information provided by the threshold photoelectron spectrum, the time-dependent breakdown curves, and the complete breakdown curve is used to explain the primary and secondary fragmentations of dimethyl ether. Ion structures are suggested where appropriate.

m/z 46

The ionization potential of 10.025 ± 0.025 eV from the threshold photoelectron spectrum can be used to calculate 0 and 298 K heats of formation (ΔH_f^0 values) for the m/z 46 $CH_3OCH_3^+$ ion. Neutral ΔH_f^0 values at 0 and 298 K for dimethyl ether are -166.293 and -184.05 kJ mol^{-1}, respectively [34]. Using these values, we calculate a $\Delta H_{f_0}^0$ ($CH_3OCH_3^+$) of 801 ± 2 kJ mol^{-1} and a $\Delta H_{f_{298}}^0$ ($CH_3OCH_3^+$) of 783 ± 2 kJ mol^{-1}. Previously reported values are 800 ± 2 kJ mol^{-1} at 0 K and 782 ± 2 kJ mol^{-1} at 298 K [23].

m/z 45

In previous studies [2,4], the $CH_3OCH_2^+$ structure has been assigned to the m/z 45 ion from dimethyl ether. The dissociation to m/z 45 is represented by the reaction

$$CH_3OCH_3^+ \rightarrow CH_3OCH_2^+ + H \qquad (1)$$

The 11.115 ± 0.010 eV threshold obtained from the fit of the 5.57 μs breakdown curve of Fig. 3 can be used with a known $\Delta H_{f_0}^0$ (CH_3OCH_3) of -166.293 kJ mol^{-1} [34] and a known $\Delta H_{f_0}^0$(H) of 216.003 kJ mol^{-1} [34] to calculate a $\Delta H_{f_0}^0$ ($CH_3OCH_2^+$) of 690 ± 1 kJ mol^{-1}. $\Delta H_{f_{298}}^0$ ($CH_3OCH_2^+$) can be calculated using the 0 K value and vibrational frequencies for the m/z 45 ion constructed from those of neutral formaldehyde and dimethyl ether [33]. Using the method outlined by Monteiro et al. [35] and the stationary electron convection [36], we calculate $\Delta H_{f_{298}}^0$ ($CH_3OCH_2^+$) to be 675 ± 1 kJ mol^{-1}.

m/z 31

The m/z 31 ion curve of Fig. 2(c) onsets at an energy $\leq 11.85 \pm 0.10$ eV and rises gradually with increasing photon energy. Both observations are in agreement with those made by Lossing [9] in an electron impact study of dimethyl ether. In that study, Lossing measured an onset for the m/z 31 ion of ≤ 11.8 eV and commented that increase in cross-section above the onset for the ion was extremely slow.

The absence of a crossover point in the breakdown curve for m/z 45 and m/z 31 below 14 eV indicates that m/z 31 is produced in a primary fragmentation. Moreover, the H_2COH^+ structure has been established in several studies [8,24,25] as the structure of this m/z 31 ion. Therefore, the dissociation of dimethyl ether$^+$ to m/z 31 can be written as

$$CH_3OCH_3^+ \rightarrow H_2COH^+ + CH_3 \qquad (2)$$

Bouma et al. [25], in a recent theoretical study, made the claim that before fragmenting to $H_2COH^+ + CH_3$, dimethyl ether$^+$ must pass over a 146 kJ mol^{-1} high energy barrier and isomerize to the $CH_3OHCH_2^+$ structure. This isomerization prior to dissociation would produce the $H_2COH^+ + CH_3$ products with 110 kJ mol^{-1} of excess energy. A conclusive test of this mechanism would be to measure the kinetic energy release in the *m/e* 31 dissociation channel as a function of the internal energy of the dimethyl ether parent ion using the coincidence experimental technique [28].

m/z 29

The *m/z* 29 ion curve of Fig. 2(b) onsets at an energy of $\leq 12.85 \pm 0.10$ eV. The only previously reported onset for this ion from dimethyl ether was 13.96 ± 0.2 eV measured in an electron impact experiment by Ivko [10]. We believe the electron impact value to be less accurate than our photoionization value due to the large energy spread of the ionizing electron beam.

The gradual rise of the *m/z* 29 curve from 12.85 to 14 eV could be produced by several thermochemically allowed processes. These include

$$CH_3OCH_3^+ \rightarrow C_2H_5^+ + OH \tag{3}$$

$$CH_3OCH_3^+ \rightarrow CH_3OCH_2^+ + H \rightarrow HCO^+ + CH_4 + H \tag{4}$$

$$CH_3OCH_3^+ \rightarrow H_2COH^+ + CH_3 \rightarrow HCO^+ + H_2 + CH_3 \tag{5}$$

$$CH_3OCH_3^+ \rightarrow H_3CO^+ + CH_3 \rightarrow HCO^+ + H_2 + CH_3 \tag{6}$$

Fortunately, several of these mechanisms can be eliminated. A high resolution mass spectral scan of the *m/z* 29 ion at nominal electron energies greater than 15 eV reveals that HCO^+ and $C_2H_5^+$ *m/z* 29 ions are produced. However, decreasing the nominal electron energy below 15 eV causes the $C_2H_5^+$ peak to disappear leaving only the HCO^+ peak. Therefore, we believe reaction (3) cannot be the source of the *m/z* 29 signal at onset. In reaction (4), the *m/z* 29 HCO^+ ion is produced in a secondary process from the *m/z* 45 fragment ion. One would expect the *m/z* 29 ion curve produced by this process to rise sharply and the *m/z* 45 curve to fall correspondingly, both curves crossing at some energy shortly above onset for the process. The fact that this behavior is not observed in Fig. 2(b) appears to rule out reaction (4). However, this is precisely what is observed from 14 to 14.9 eV and is presumed to be the source of the crossover observed there (see below). In reaction (5), the HCO^+ ion is again produced in a secondary process from the H_2COH^+ *m/z* 31 ion. As in the case of reaction (4), the rise of the *m/z* 29 ion curve does not correspond to a fall in the *m/z* 31 curve. In fact, the *m/z* 31 curve continues to slowly rise above the onset of the *m/z* 29 ion

indicating that H_2COH^+ is not the source of the m/z 29. The AE(298) of HCO^+ produced in reaction (5) can be calculated from the $\Delta H^0_{f_{298}}$ values of HCO^+ (816 kJ mol^{-1}), CH_3 (142.3 kJ mol^{-1}), and CH_3OCH_3 (-184.05 kJ mol^{-1}) [34] and a knowledge of the height of the reverse activation barrier (125 kJ mol^{-1}) for the 1,2-hydrogen elimination reaction [37]. The AE(298) is determined to be 13.14 ± 0.15 eV. It is tempting on the basis of this calculation to attribute the m/z 29 signal below 14.0 eV to reaction (5) alone. However, the onset for m/z 29 of $\leq 12.85 \pm 0.010$ eV measured from the breakdown curve is lower than that which is thermochemically calculated. This behavior is contrary to the effects of kinetic and competitive shifts on experimentally determined onsets. Despite the apparent absence of a decrease in the m/z 31 curve below 14.0 eV, we believe that reaction (5) could occur at energies ≥ 13.14 eV. The anticipated decrease could be spread over several electron volts and displaced to higher energies due to (1) the broad internal energy distribution [38] of the reacting H_2COH^+ ions and (2) the fact that reaction (5) has been shown to be a metastable process [37,39]. Perhaps the decrease in the m/z 31 curve above 14.5 eV is due to reaction (5) and the increasing m/z 15 curve. This can certainly be checked by a careful modeling of the reaction and a subsequent calculation of the breakdown curve. In reaction (6), the HCO^+ ion is produced in a secondary reaction from the isomeric m/z 31 H_3CO^+ methoxide ion. Bowen and Williams [26] have observed that the 70 eV mass spectrum of dimethyl ether has no discernible metastable peak for the dissociation of H_3CO^+ to $HCO^+ + H_2$. This was attributed to a small activation energy and fast rise of the rate versus energy curve for the reaction. The claim of a fast reaction of H_3CO^+ to $HCO^+ + H_2$ was further substantiated by the results of a collisional activation study by Dill et al. [24]. In this experiment, comparison of the collisional activation of m/z 31 ions produced from dimethyl ether and 9 other precursors indicated that only one m/z 31 isomer, H_2COH^+, existed 10^{-5} s after ion formation. The possibility was suggested, however, that at higher energies the H_3CO^+ ion could be formed as a result of direct bond cleavage from dimethyl $ether^+$. The inability to detect a collisional activation spectrum for the H_3CO^+ ion could be explained as being due to the fast reaction ($k > 10^5$ s^{-1}) of the H_3CO^+ ion to $HCO^+ + H_2$. The tendency for the H_3CO^+ to dissociate to $HCO^+ + H_2$ is further reflected in the gas phase equilibrium studies of Hiraoka and Kebarle [40,45]. In these experiments, the H_3CO^+ ion produced by combining H_2 and HCO^+ in a high-pressure pulsed mass spectrometer was found to be stable only at temperatures less than 100°C. At higher temperatures, H_3CO^+ reverts to the products $HCO^+ + H_2$. The fact that the H_3CO^+ ion rapidly dissociates to HCO^+ and H_2 enables us to explain the source of the m/z 29 signal below 14 eV as being due principally to reaction (6). We believe that the H_3CO^+ ion is formed

from dimethyl ether$^+$ in a direct dissociation. The H_3CO^+ ion then rapidly dissociates to HCO^+ and H_2. In coincident time-of-flight spectra recorded near the 12.85 eV onset, the m/z 29 HCO^+ ion peaks did not exhibit tails to longer time-of-flight characteristic of metastable dissociations [30]. This means that the primary and secondary steps of reaction (6) must occur with rates $\geq 10^7$ s^{-1}. Therefore, H_3CO^+ ions dissociate to HCO^+ and H_2 as quickly as they are formed, causing no decrease in the m/z 31 ion curve below 14 eV.

From 14.0 to 14.9 eV, the m/z 29 breakdown curve rises sharply. This rise in the m/z 29 signal corresponds nicely with the abrupt fall in the m/z 45 curve indicating that, in this energy range, m/z 29 is being formed from m/z 45 according to reaction (4). Hvistendahl and Williams [41] determined the activation energy for CH_4 loss from $CH_3OCH_2^+$ to be ≤ 347 kJ mol^{-1}. Using the onset of 14.0 ± 0.1 eV from the breakdown curve as a measure of the AE(298) produces a calculated activation energy of ≤ 285 kJ mol^{-1}.

At photon energies greater than 14.90 eV, the m/z 29 curve slowly decreases due to the increasing rate of the competing m/z 15 dissociation channel. The decrease in m/z 29 curve could also be attributed, to a lesser extent, to the production not only of HCO^+, but also $C_2H_5^+$ and possibly COH^+ ions, all of which have large amounts of kinetic energy [42].

The production of the $C_2H_5^+$ m/z 29 ion detected by high resolution mass spectrometry at nominal electron greater than 15 eV is intriguing. It is difficult to pinpoint the exact source of this ion at these energies. Determination of the precursor to $C_2H_5^+$ is complicated by the number of thermochemically accessible isomers of m/z 31, m/z 45, and m/z 46. One possibility is that the $C_2H_5^+$ ion could be formed in a fast dissociation from the m/z 45 $C_2H_5O^+$ ethoxide ion isomer. To date, the ethoxide ion has been detected only in a charge stripping experiment [43]. At this stage, determination of the source of $C_2H_5^+$ at high energies is contingent upon further experimentation.

Several electron impact mass spectrometric studies have reported large m/z 29 ion signals from dimethyl ether [10,26,44]. According to the breakdown curve of Fig. 2(b) and (c), the m/z 29 ion should also be an abundant fragment in the photoionization mass spectrum of dimethyl ether. It is puzzling that in the photoionization mass spectrometric study of dimethyl ether by Botter et al. [23], no mention was made of a m/z 29 fragment ion. However, their photoionization efficiency curve for m/z 31 from dimethyl ether has an onset at approximately the same energy as the m/z 29 breakdown curve in Fig. 2(b). Moreover, the m/z 31 photoionization efficiency curve measured by Botter et al. exhibits definite changes in slope at precisely the same energies as the changes in slope of our m/z 29 breakdown curve. A reasonable explanation would be that the m/z 31 photoionization

curve was misidentified in the photoionization study and is, in reality, m/z 29.

m/z 15

An AE(298) of 14.4 ± 0.1 eV can be measured from the m/z 15 CH_3^+ ion curve. This is in precise agreement with the value of 14.4 eV measured by Botter et al. [23]. The m/z 15 CH_3^+ ion is formed in a secondary ion dissociation from the m/z 45 according to the reaction

$$CH_3OCH_3^+ \rightarrow CH_3OCH_2^+ + H \rightarrow CH_3^+ + H_2CO + H \qquad (7)$$

SUMMARY

An AE(0 K) of 11.115 ± 0.010 eV for the dissociation of dimethyl ether to m/z 45 is obtained from a calculated fit of the crossover region of the m/z 45 and m/z 46 ion curves at 5.57 μs ion residence time. Using this threshold, the heat of formation of $CH_3OCH_2^+$ at 0 and 298 K is calculated to be 690 ± 1 and 675 ± 1 kJ mol^{-1}, respectively.

Information from the breakdown curve is used to determine the primary and secondary fragmentations of dimethyl ether$^+$. Primary fragmentations include

$$CH_3OCH_3^+ \rightarrow \underset{(m/z\ 45)}{CH_3OCH_2^+} + H$$

$$CH_3OCH_3^+ \rightarrow \underset{(m/z\ 31)}{H_2COH^+} + CH_3$$

Secondary fragmentations include

$$CH_3OCH_3^+ \rightarrow H_3CO^+ + CH_3 \xrightarrow{\text{fast}} \underset{(m/z\ 29)}{HCO^+} + H_2 + CH_3 \qquad (\leq 12.85\ \text{eV})$$

$$CH_3OCH_3^+ \rightarrow CH_3OCH_2^+ + H \rightarrow \underset{(m/z\ 29)}{HCO^+} + H + CH_4 \qquad \text{(high energy)}$$

$$CH_3OCH_3^+ \rightarrow H_2COH^+ + CH_3 \xrightarrow{\text{slow}} \underset{(m/z\ 29)}{HCO^+} + H_2 + CH_3 \qquad (\geq 13.14\ \text{eV})$$

$$CH_3OCH_3^+ \rightarrow CH_3OCH_2^+ + H \rightarrow \underset{(m/z\ 15)}{CH_3^+} + H_2CO + H$$

A detailed modeling of the full breakdown curves will be published elsewhere.

ACKNOWLEDGEMENTS

We would like to thank Dr. Edward White, V for providing us with the high resolution mass spectral data. Sincere thanks are also extended to Professors John Holmes and Joel Liebman for their valuable insight into the dimethyl ether problem.

We are indebted to the late Dr. Henry Rosenstock for originally suggesting the study of this problem.

NOTE ADDED IN PROOF

Recently, Burgers and Holmes [46] have measured the $\Delta H^{\circ}_{f_{298}}$ of triplet H_3CO^+ experimentally to be 1034 ± 20 kJ mol^{-1}. Using this value, the AE(298) for HCO^+ according to reaction (6) is calculated to be 14.1 eV. If this is true, reaction (6) cannot be the source of m/z 29 below 14.0 eV. In the same series of experiments, the H_2COH^+ and H_3CO^+ ions were found to eliminate H_2 through a common transition state. This implies that HCO^+ produced by reaction (5) should appear at energies greater than 14.1 eV. In the light of these results, the source of m/z 29 below 14.0 eV in photoionization experiments remains a puzzle.

REFERENCES

1 G.J. Hernandez, J. Chem. Phys., 38 (1963) 1644.
2 R.H. Martin, F.W. Lampe and R.W. Taft, J. Am. Chem. Soc., 88 (1966) 1353.
3 S. Tsuda and W.H. Hamill, Adv. Mass Spectrom., 3 (1966) 249.
4 A.G. Harrison, A. Ivko and D. van Raalte, Can. J. Chem., 44 (1966) 1625.
5 A.B. King and F.A. Long, J. Chem. Phys., 29 (1958) 374.
6 R.R. Bernecker and F.A. Long, J. Phys. Chem., 65 (1961) 1565.
7 M.S.B. Munson and J.L. Franklin, J. Phys. Chem., 68 (1964) 3191.
8 M.A. Haney and J.L. Franklin, Trans. Faraday Soc., 65 (1969) 1794.
9 F.P. Lossing, J. Am. Chem. Soc., 99 (1977) 7526.
10 A.A. Ivko, Org. Katal., (1970) 20.
11 K. Watanabe, T. Nakayama and J. Mottl, J. Quant. Spectrosc. Radiat. Transfer, 2 (1962) 369.
12 K. Watanabe, J. Chem. Phys., 26 (1957) 542.
13 M.J.S. Dewar and S.D. Worley, J. Chem. Phys., 50 (1969) 654.
14 B.J. Cocksey, J.H.D. Eland and C.J. Danby, J. Chem. Soc. B, (1971) 790.
15 S. Cradock and R.A. Whiteford, J. Chem Soc. Faraday Trans. 2, 68 (1972) 281.
16 D.H. Aue, H.M. Webb and M.T. Bowers, J. Am. Chem. Soc., 97 (1975) 4137.
17 F.M. Benoit and A.G. Harrison, J. Am. Chem. Soc., 99 (1977) 3980.
18 T. Kobayashi, Phys. Lett. A, 69 (1978) 105.
19 H. Bock, P. Mollere, G. Becker and G. Fritz, J. Organometal. Chem., 61 (1973) 113.
20 D.H. Aue, H.M. Webb, W.R. Davidson, M. Vidal, M.T. Bowers, H. Goldwhite, L.E. Vertal, J.E. Douglas, P.A. Kollman and G.L. Kenyon, J. Am. Chem. Soc., 102 (1980) 5151.

21 C. Utsunomiya, T. Kobayashi and S. Nagakura, Bull. Chem. Soc. Jpn., 53 (1980) 1216.
22 F. Carnovale, M.K. Livett and J.B. Peel, J. Am Chem. Soc., 102 (1980) 569.
23 R. Botter, J.M. Pechine and H.M. Rosenstock, Int. J. Mass Spectrom. Ion Phys., 25 (1977) 7.
24 J.D. Dill, C.L. Fischer and F.W. McLafferty, J. Am. Chem. Soc., 101 (1979) 6531.
25 W.J. Bouma, R.H. Nobes and L. Radom, Org. Mass Spectrom., 17 (1982) 315.
26 R.D. Bowen and D.H. Williams, J. Chem. Soc. Chem. Commun., (1977) 378.
27 J.L. Holmes, F.D. Lossing, J.K. Terlouw and P.C. Burgers, J. Am. Chem. Soc., 104 (1982) 2931.
28 R.L. Stockbauer, Int. J. Mass Spectrom. Ion Phys., 25 (1977) 89.
29 R.L. Stockbauer and H.M. Rosenstock, Int. J. Mass Spectrom. Ion Phys., 27 (1978) 185.
30 H.M. Rosenstock, R.L. Stockbauer and A.C. Parr, J. Chem. Phys., 71 (1979) 3708.
31 K. Kimura, S. Katsumata, Y. Achiba, T. Yamazaki and S. Iwata, Handbook of HeI Photoelectron Spectra of Fundamental Organic Molecules, Halsted Press, New York, 1981.
32 H.M. Rosenstock, R. Buff, M.A.A. Ferreira, S.G. Lias, A.C. Parr, R.L. Stockbauer and J.L. Holmes, J. Am. Chem. Soc., 104 (1982) 2337.
33 T. Shimanouchi, NSRDS-NBS 39, 1972.
34 H.M. Rosenstock, K. Draxl, B.W. Steiner and J.T. Herron, J. Phys. Chem. Ref. Data, Suppl. 6 (1982) 1.
35 M.L. Fraser-Monteiro, L. Fraser-Monteiro, J.J. Butler, T. Baer and J.R. Hass, J. Phys. Chem., 86 (1982) 739.
36 H.M. Rosenstock, in P. Ausloos (Ed.), Kinetics of Ion–Molecule Reactions, Plenum Press, New York, 1979, pp. 246–249.
37 J.L. Holmes and J.K. Terlouw, Org. Mass Spectrom., 15 (1980) 383.
38 M.B. Wallenstein and M. Krauss, J. Chem. Phys., 34 (1961) 929.
39 D.H. Williams and G. Hvistendahl, J. Am. Chem. Soc., 96 (1974) 6753.
40 K. Hiraoka and P. Kebarle, J. Chem. Phys., 63 (1975) 1688.
41 G. Hvistendahl and D.H. Williams, J. Am. Chem. Soc., 97 (1975) 3097.
42 R. Stockbauer, J. Chem.. Phys., 58 (1973) 3800.
43 M.M. Bursey, J.R. Hass, D.J. Harvan and C.E. Parker, J. Am. Chem. Soc., 101 (1979) 5485.
44 S.R. Heller and G.W.A. Milne, EPA/NIH Mass Spectral Data Base, Vol. 1, NSRDS – NBS 63, U.S. Government Printing Office, Washington, DC, 1978.
45 K. Hiraoka and P. Kebarle, J. Am. Chem. Soc., 99 (1977) 366.
46 P.C. Burgers and J.L. Holmes, Org. Mass Spectrom., submitted for publication.